Carbohydrate Polymers 78 (2009) 978–986

Contents lists available at ScienceDirect

Carbohydrate Polymers

journal homepage: www.elsevier.com/locate/carbpol

Molecular dynamics simulations of a cyclic-DP-240 amylose fragment in a periodic cell: Glass transition temperature and water diffusion

Frank A. Momany *, J.L. Willett, Udo Schnupf

Plant Polymer Research Unit, [1]USDA, ARS, MWA, National Center for Agricultural Utilization Research, 1815 N. University St., Peoria, IL 61604, USA

ARTICLE INFO

Article history:
Received 21 October 2008
Received in revised form 13 July 2009
Accepted 17 July 2009
Available online 23 July 2009

Keywords:
Glass transition temperature
Molecular dynamics
c-DP-240
Self diffusion coefficient

ABSTRACT

Molecular dynamics simulations using AMB06C, an in-house carbohydrate force field, (NPT ensembles, 1 atm) were carried out on a periodic cell that contained a cyclic 240 glucose residue amylose fragment (c-DP-240) and TIP3P water molecules. Molecular conformation and movement of the amylose fragment and water molecules at different temperatures were examined. The periodic cell volume, density, and potential energy were determined at temperatures above and below the glass transition temperature (T_g) in 25 K increments. The amorphous cell is constructed through successive dynamic equilibration steps at temperatures above the assumed T_g value and the temperature successively lowered until several temperature points were obtained below T_g. Molecular dynamics simulations were continued for at least 500 ps or until the volume drift stopped and remained constant for several hundred picoseconds. The T_g values were found by noting the discontinuity in slope of the volume (V), potential energy (PE), or density (ρ) versus $1/T$. The changes in flexibility and motion of the amylose chain as well as differences in self diffusion coefficients of water molecules are described. The final average T_g value found (316 K) is in agreement with experimental values, i.e. ~320 K.

Published by Elsevier Ltd.

1. Introduction

In a previous study, (Momany & Willett, 2002) the methodology for computational studies of glass transition (T_g) temperatures of ten DP-10 amylose fragments was described. It was shown in that particular study that the thermal expansivity decreased as it passed from the rubbery to the glassy state at T_g. In the computational work described here, glass transition temperature and diffusion studies are carried out on one large amylose fragment. The fragment consists of 240 glucose residues which are $^4C_1$ and α-(1 → 4) linked forming a cyclic-DP-240 (c-DP-240), to simulate an amorphous amylose molecule. Experimental determination of 3-dimensional amorphous carbohydrate structures is complicated since X-ray diffraction and NMR spectra provide conflicting structural information, with some repeating patterns showing up in the NMR and different patterns in the X-ray results. Computational simulations allow us to examine this experimental dilemma in some detail, looking at the different micro-structural components and molecular motions of the polymer and solvent.

Experimental studies on amylose fragments have been carried out to determine the glass transition temperature, with results suggesting a range in T_g values from ~310 K for maltohexaose (Orford, Parker, Ring, & Smith, 1989) to ~330 K for wet amylose and amylopectin, and well into the 400–500 K range for low hydration studies (Shogren, 2000). Temperatures near room temperature are reasonable ones for molecular mechanics simulations such as those reported here (Momany & Willett, 2000a, 2000b, 2002).

Computational methods applied to carbohydrates have received considerable attention recently, with work directed toward monosaccharides (Howard & Grigera, 1992; Caffarena & Grigera, 1997; Caffarena & Grigera, 1999; Hajduk, Horita, & Lerner, 1993), disaccharides (Ekdawi-Sever, Conrad, & de Pablo, 2001; Parker & Ring, 1995; Tromp, Parker, & Ring, 1997; Perico et al., 1999; Yoshioka & Aso, 2005; Simperler et al., 2007) and other saccharides (Braesicke, Steiner, Saenger, & Knapp, 2000; Roberts & Debenedetti, 1999; Stevensson et al., 2000; Trommsdorff & Tomka, 1995a; Trommsdorff & Tomka, 1995b; Shimada, Kaneko, Takada, Kitamura, & Kajiwara, 2000; Lee & Debenedetti, 2005). To our knowledge, no studies of the size molecule examined here have been carried out using an atomic based force field. NMR studies of interest to this question have also been carried out, primarily on small molecules (Kullik, Chris de Costa, & Haverkamp, 1994; Maler, Widmalm, & Kowalewski, 1996; Tang, Godward, & Hills, 2000).

The T_g values determined here are compared to those obtained from native starch materials at similar hydration concentration, and the mobility and clustering capability of the water molecules are described. A comparison of the calculated self diffusion coeffi-

* Corresponding author. Tel.: +1 309 681 6362.
E-mail address: frank.momany@ars.usda.gov (F.A. Momany).

[1] Names are necessary to report factually on available data; however, the USDA neither guarantees nor warrants the standard of the product, and the use of the name by USDA implies no approval of the product to the exclusion of others that may also be suitable.

0144-8617/$ - see front matter Published by Elsevier Ltd.
doi:10.1016/j.carbpol.2009.07.034

cients is made to that of pure water at different temperatures. Analysis of the water translational and rotational motion is described, as well as cluster sizes and interactions with the carbohydrate.

2. Computational methods and molecule preparation

Molecular mechanics and dynamic simulations were carried out using the software package InsightII/DISCOVER (version 2000.3L, InsightII/Discover, Accelrys Corp.) Energy minimization and dynamics were performed using our newly developed all atom force field, AMB06C, [see Appendix for force field parameters and test of force field on a cyclic 26-mer fragment of known molecular structure], within the InsightII/DISCOVER program. All simulations were carried out on an IBM IntelliStation M Pro workstation. A rectangular cell ($\sim$41 Å $\times$ 41 Å $\times$ 37 Å) with periodic boundaries was constructed such that the c-DP-240 fragment of amylose plus water molecules could be completely enclosed within a periodic cell, containing a limited number of vacuum holes. Non-bonded interaction cutoffs were set at 15 Å with a spline window width of 2 Å. A dielectric constant value of one was used. There are no charged groups (only partial charges reside on the glucose residues and water molecules) in the system studied, and long range convergence methods were not found to be necessary with 15 Å cutoffs, considering that the energy differences would be very small. The TIP3P water model was used similarly to the authors studies on the solution dynamics of maltose and several cyclodextrins (Momany & Willett, 2000a; Momany & Willett, 2000b). All molecules within the system were studied with the all atoms potentials (no group potentials were used) and were considered to be fully flexible during energy minimization and molecular dynamics simulations.

The procedure used to construct the amorphous cell included the following steps: First, a DP-240 chain was constructed from DP-20 segments of α-D-glucose units using the Polymerizer program in InsightII. Atom types, potentials, and partial atomic charges (see Appendix) were assigned to every atom using the atom types and new partial charges found from the development of AMB06C, a modified AMBER force field based on the previously published (AMB99C) (Momany & Willett, 2000a; Momany & Willett, 2000b) force field for carbohydrates. An example test case of the revised force field is provided in the Appendix. The initial single chain backbone dihedral angles for the DP-20 oligomers were those which would create a helical *syn* orientation (defined using the H1, and H4' hydrogen atoms; $\phi_H \sim 0^o$, $\psi_H \sim 0^o$), a band-flip ($\phi_H \sim 0^o$, $\psi_H \sim 180^o$), or kink ($\phi_H \sim -40^o$, $\psi_H \sim -50^o$)(Gessler et al., 1999), or a more random conformation with backbone dihedral angles within 10°–15° of the DFT calculated α-maltose minimum energy positions (Momany, Schnupf, Willett, & Bosma, 2007; Momany & Willett, 2000c). Different conformations of segments of DP-20 were generated and allowed to undergo dynamic simulation *in vacuo* for 100 ps to find an overall conformation in which every set of backbone dihedral angles was in the range described above. Side-chain hydroxymethyl groups were randomly placed on each chain as either gg (*gauch* to both C4 and O5) or gt (*gauch* to O5, trans to C4), ($\sim$50/50%) and the side-chain placements allowed different equilibrated conformations to be created as the vacuum dynamics proceeded. The so obtained DP-20 fragments were then linked to obtain longer fragments, ultimately c-DP-240. As each DP-20 segment was added, the cluster was refined by adjusting the dihedral angles of the chains to create the smallest rectangular structure possible without creating atomic overlaps. This process required the addition of numerous band-flip conformations to complete the structure. Clearly, this process does not produce a unique structure, but only one structure out of a practically unlimited number of structures, as would be expected of an amorphous polymer.

It is of interest to note that in the preliminary simulations it was observed that the two ends of a linear DP-240 chain were difficult to control, moving during dynamics out into adjacent image cells (threading between the image structures). The simulation methods were not able to be completed when the chains moved to $\sim$1/2 of the cell dimension into an adjacent cell. To prevent this migration of the chain ends, it was possible to add constraining distance potentials to the end groups and slowly during several dynamics runs, bring the two ends of the DP-240 residue chain close to one another. The end groups were then treated through the InsightII builder and fused together through a $\alpha(1 \rightarrow 4)$ bridge to complete the cyclic chain structure. This cyclization process produced a stable system that did not unravel and migrate significantly into the adjacent cells. From this point on we denote the cyclic form, c-DP-240. All results presented are for the cyclic structure.

A periodic cell was next constructed around the molecule and TIP3P water molecules added into the void spaces within the cell. The periodic cell was carried through a series of NVT and NPT dynamic simulations, of $\sim$500 ps duration to achieve pseudo-equilibrated conditions. In the first simulations it was found that the hydration level was too large. That is, the cell was very large, the density was relatively low, and in order to lower the volume of the cell, water molecules were randomly removed from the cell. The equilibration steps were again repeated allowing the cell to shrink accordingly in order to reach a desired hydration level ($\sim$13%) plus the c-DP-240 molecule. The final cell dimensions were the result of many steps as described above (297 water molecules, $\sim$13%) and reasonable density. Time steps for integrations were 1 fs and velocities, volumes, and pressures were collected every 1 ps. Initial temperatures studied were in the 250–400 K range since the T_g of starch at $\sim$13% hydration is known experimentally to be in the range, 315–350 K. Preliminary examination of the volume and potential energy plotted as a function of time showed that simulations of the order of $\sim$500 ps would be required before both the volume and potential energy remained constant with time at each temperature. For this reason, more than 5 ns of NVT dynamics simulation was carried out at 300 K prior to reaching a cell considered to be near equilibration. After each $\sim$500 ps simulation, the complex was energy minimized to $\sim$0.01 gradient using the conjugate gradient method and an attempt was made to add new water molecules to the cell to increase the density. This procedure was carried out multiple times, and only after no new water molecules could be added was the first NPT simulation started. Initially, slightly less than one atmosphere (0.8 atm) was used for the pressure control during preliminary NPT simulations, moving to 1 atm for the final runs. Holding the pressure constant the temperature was increased from 250 K to 400 K in 25 K increments. Next, the direction was reversed and the temperature decreased by the same increments down to 250 K. This criteria for constant cell structure was used for simulations at each temperature, in particular the results of three runs were required to give the same or close average volume without up or down drift in the volume over the time of the run. After reaching the desired equilibrium, the simulation for that temperature was considered complete. Moving down in temperature the volume of the cell gets smaller and the final volume measurements for each temperature could be made. For one hydration level the mass remains constant for every NPT simulation even though the volume changes with change in temperature, in this way the average density or specific volume is obtained.

It was observed during early simulations, particularly those at higher temperatures, i.e. 375–400 K, that the ring conformation of selected residues could distort from the chair ($^4C_1$) form into a twisted pseudo boat or skew form. This was particularly true dur-

ing the preliminary simulations when close contacts were found, a result of packing the molecule in an ever smaller cell as water was removed, and when using distance constraints to hold loops and extended sections of molecule inside the cell. This transition was not predictable and occurred at random locations in the c-DP-240 fragment. When these structural transitions were found, a constraining torsional potential was applied to the residue ring atoms, C5–O5–C1–O1 and/or O2–C2–C3–O3 with a torsional potential constant of 1000 kcal/mol-deg and a dihedral angle of ~60°. Upon energy minimization and further molecular dynamics the distorted rings returned to their normal chair conformation, and the constraining potentials removed.

An in-house analysis program was used to find and help correct any discrepancies in the structure, analyze water clusters sizes and their populations, determine hydroxymethyl populations, clockwise, 'c', and counterclockwise, 'r', hydroxyl rotamer populations, band-flip numbers, and other parameters reported here.

Plots of equilibrated volume, potential energy, or density vs. the reciprocal of the temperature ($1/T$) result in two lines of differing slope, one line for data above and one for data below the T_g value. Least squares analysis of these lines is carried out, and upon solving the two simultaneous equations the crossing point (i.e. T_g) is determined.

3. Diffusion

The measure of the path and time scale for water molecules to move through the amylose matrix can be characterized by evaluating the spatially dependent self diffusion constant and the main diffusion direction of the MD simulation data. The calculation of the mean square displacement (MSD) is of interest as it leads to the determination of the self diffusion coefficient of an atom or molecule. That is, as the dynamic simulation proceeds over time, the position of an atom or molecule in the periodic system changes relative to its coordinate position at the start of the simulation. Thus, knowing the position vector of the atom and averaging over all choices of time origin within a dynamics trajectory, one can obtain the MSD. The self diffusion coefficient (D_T) is then defined as follows:

$$D_T = (1/6)\lim(t \leftarrow \infty) d[\mathrm{MSD}]/dt. \quad (1)$$

D_T is evaluated from the limiting slope of the MSD from a plot of MSD vs. time for the particular dynamics simulation. The middle time regions of the plotted data have reasonably constant slope, and this region is used to obtain values of the diffusion coefficient. The slope units are in $Å^2/ps^{-1}$ and can be converted to m^2/s^{-1} in order to compare them with experimental values. Eq. (2) allows the calculation of the activation energy (ΔE) for the diffusion of water.

$$D_T = D_0\, e^{-(\Delta E/RT)} \quad (2)$$

R is the universal gas constant and T the temperature. The natural log plot of Eq. (2) gives the activation energy.

To obtain an expression for the diffusion pathway for an individual water molecule during dynamic simulations is difficult. One method for calculating interaction lifetimes (Astley, Birch, Drew, & Rodgers, 1999) is used in part here. In particular, the position of the water molecule is probed as a function of time using two slowly moving carbohydrate chain atoms as distance parameters. Because of the difference in mass the carbohydrate chains have smaller amplitudes of motion and are moving much slower than the water molecules. This can be seen by the difference in MSD. Thus, by choosing for example, two oxygen bridging or ring atoms separated in space by at least one glucose ring unit, one can plot the distance from the water oxygen (or hydrogen) to both reference oxygen atoms as a function of time for the particular dynamics simulation. In practice it is preferential to use oxygen atoms that are on different chains and separated from the water of interest. It is relatively straight forward to find those water molecules that are moving about the cell, by examination of all the water molecules during the time dependent dynamics as shown visually and by analysis of the distance each water molecule moved during the simulation. Those water molecules that move in "jump-like" steps or migrate slowly to different positions in the cell during the dynamics are examined using distance functions.

4. Results and discussion

The results of the molecular dynamics simulations of the c-DP-240 amylose in a periodic cell at ~13% hydration are presented in Tables 1 and 2, and Figs. 1 through 8. Table 3 gives the diffusion coefficients for the temperature range studied.

Table 1 gives three sets of parameters for the density (ρ), volume (V), and potential energy (PE) at different temperatures spanning the temperature range above and below T_g. Several obvious features in Table 1 stand out. First, as the temperature increases, the volume of the cell increases and the potential energy increases. The density, which is inversely proportional to the volume, decreases. In Fig. 1 is shown the plot of the average values of ρ, V, and PE against $1/T$. Second, at the higher temperatures the slope of the line is greater than at lower temperatures, showing that

Table 2
Calculated and experimental glass transition temperatures, T_g(K), of c-DP-240 at 13% hydration.

	c-DP-240
T_g from potential energy	314.9
T_g from volume	319.4
T_g from density	314.1
Average T_g	316.1
Experimental T_g	315–340[a]

[a] 325 K estimated from Fig. 2 of Orford et al. (1989) for maltohexaose; 315 K estimated from Fig. 3 of Orford et al. (1989) for DP-10 chains at 13% hydration; 340 K estimated for starch from Fig. 4 of Shogren (2000).

Table 1
Potential energy (PE), volume (V), and density (ρ) of c-DP-240 for simulations at temperatures of 250 K to 375 K.

	Set #1			Set #2			Set #3			Average[b]		
Temp[a]	PE[a]	V[a]	ρ[a]	PE	V	ρ	PE	V	ρ	PE	V	ρ
250	14428	55385	1.326	14392	55317	1.328				14410	55351	1.327
275	14970	55383	1.326	14902	55503	1.324	14881	55448	1.325	14918	55445	1.325
300	15490	55615	1.321	15455	55526	1.323	15371	55674	1.320	15439	55605	1.322
325	15958	55774	1.317	15950	55809	1.316	15886	55819	1.316	15931	55800	1.316
350	16530	56158	1.308	16439	56247	1.306	16394	56017	1.311	16454	56141	1.308
375	16927	56417	1.302	16953	56586	1.298	17090	56835	1.293	16990	56612	1.298

[a] Potential Energy units are kcal/mol, volume units are Å3, and density units are g/cm^3.
[b] Average values over all sets.

Table 3
Self diffusion coefficients (D_T) of c-DP-240 for the solvent hydration level of 13% water[a], as a function of temperature.

Temperature, K	c-DP-240		Water	
	Slope, Å^2/ps	D_T	Slope, Å^2/ps	D_T
250	0.000125	0.00002	0.110	0.019
275	0.00020	0.00003	0.123	0.020
300	0.00029	0.00005(5×10^{-9}/cm^2/s)	0.235	0.039
325	0.00044	0.00007	0.386	0.064
350	0.00089	0.00015	0.378	0.063
375	0.00155	0.00026	0.397	0.066

[a] Self diffusion coefficients of water at 275, 300, and 325 K are 0.12, 0.23, and 0.36 Å^2/ps respectively (Mills, 1973). Pure water is 0.189 Å^2/ps while 80% sucrose solution at 400 K (Ekdawi-Sever et al., 2001) gives a value of $D_T \sim 9 \times 10^{-8}$/cm^2/s.

the coefficient of expansion is greater at temperatures above T_g. The intersection of the two least squares lines is the glass transition temperature denoted, T_g. Table 2 gives the resulting T_g values obtained using data from Table 1.

In order to analyze the conformations of each residue in the c-DP-240 amylose a software analysis package was developed which recognizes the different ring conformations, side-chain hydroxyl group conformations, hydroxymethyl conformation, and flipping of the glycosyl rings at the bridging ether. The analysis for the final 350 K run provides the following information; 57 band-flips, 8 kink conformations, 109 gg residues, 125 gt residues, and 6 tg bearing residues. All glycosyl residues retained their $^4C_1$ chair conformation. A final run at 250 K resulted in 55 band-flips, 9 kink conformations, 107 gg, 126 gt, and 7 tg residues. As above, all residues retained their $^4C_1$ ring conformation. The large number of band-flips is a result of the folding required to fit into a periodic cell size that was required to achieve a level of computation compatible with the resources available. The distribution of hydroxymethyl conformations is only slightly biased toward gt, whereas the starting population was 50/50%.

In Fig. 2 is shown a figure of a packed cell of c-DP-240 and the 297 water molecules as distributed evenly throughout the cell. The conformation shown in Fig. 2 resulted from ~1.5 ns of molecular dynamics at 300 K and is a snapshot at 500 ps of the run in which 297 water molecules are included. Analysis of the water clusters at two different temperatures, 250 K and 350 K shows a makeup of 62 and 75 monomer water molecules, 26 and 15 dimers, 11 and 8 trimers, 3 and 3 tetramers, 3 and 2 pentamers, 2 and 3 hexamers, and 1 and 1 decamers respectively for the two temperatures. There are few clusters larger than a decamer. The largest clusters found consisted of 29 water molecules appear at lower temperatures and similarly, 25 water molecule clusters occur at higher temperatures. A water cluster is defined as that combination in which each water molecule is hydrogen bonded to at least one other water molecule (H···O less than 2.5 Å, and reasonable H···O–H angle between water molecules). The result of this analysis is that most of the water molecules are in contact with the c-DP-240 regardless of the temperature. Water can act as donor and acceptor to form hydrogen bonds. Waters are rarely found in the glycosidic bond region or interacting with the ring oxygen of the glucose residues. As one would expect water interacts most frequently with the H–O6 atoms of the carbohydrate residues and somewhat less with the H–O2 and H–O3 atoms.

Single water molecules are described as they are important in stabilizing interactions between different segments of the amylose chain. Two different types of "bridging" water molecules are shown in Fig. 3. In Fig. 3a one water molecule is interacting with the H–O2 and O3–H groups of one residue, and at the same time forming a "bridge" to an H–O6 group of a second glucose residue located on a different amylose chain. In Fig. 3b a "bridging" water molecule is shown interacting with two O6 groups located in consecutive residues on one chain, with an O2 oxygen atom located on a different chain. It appears that "bridging" interactions can occur with ease between any of the hydroxyl groups of a residue on one chain with those on another chain. The effect of stabilizing the chain–chain interactions with "bridging" water molecules is significant in energy even though the hydrogen bond lengths can be sometimes fairly large, ~2–3 Å in H···O distance.

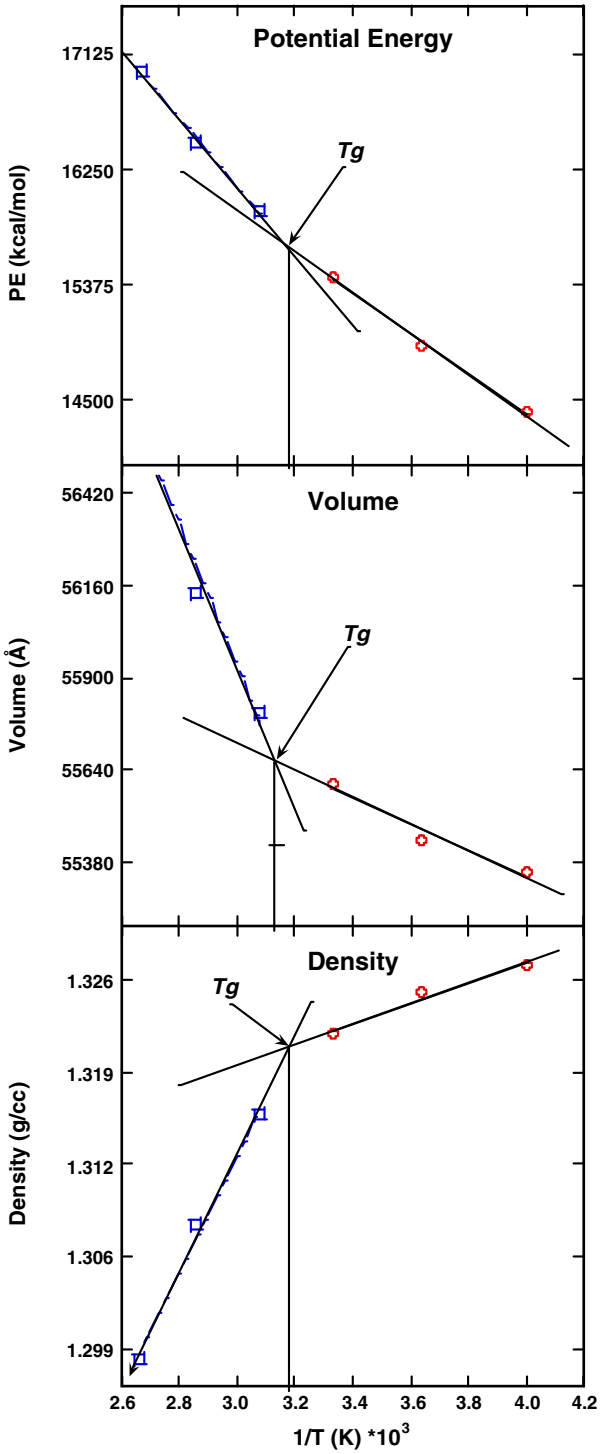

Fig. 1. Plot of average values of potential energy, volume and density as a function of inverse temperature for c-DP-240 (data taken from Table 1).

In Fig. 4a is shown one tetramer water cluster. The hydrogen bond lengths are around 1.9 Å, in good agreement with experimental hydrogen bond lengths. In the case shown, one water molecule

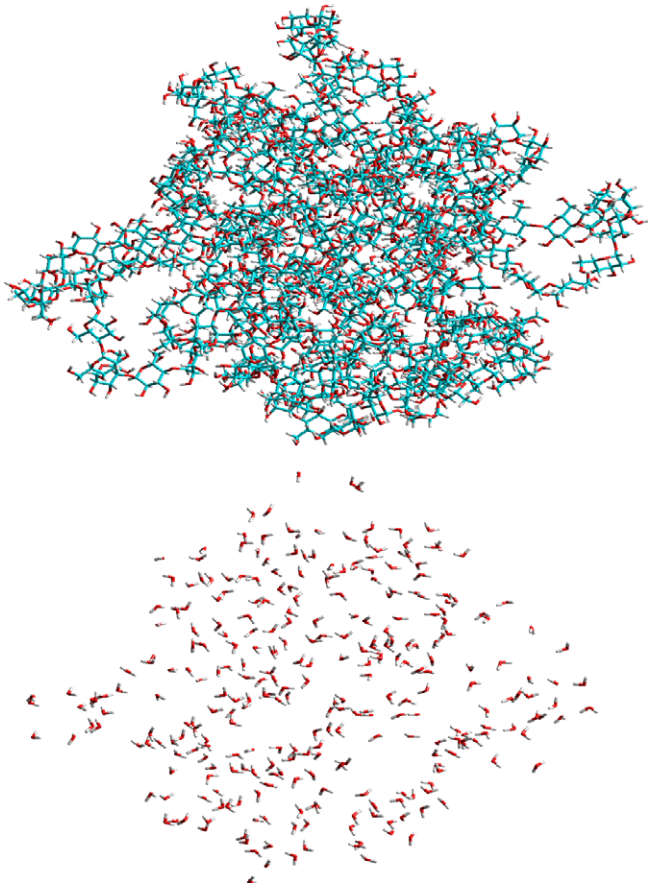

Fig. 2. Stick figure of the c-DP-240 (top) and 297 water molecules (bottom) in a packed cell.

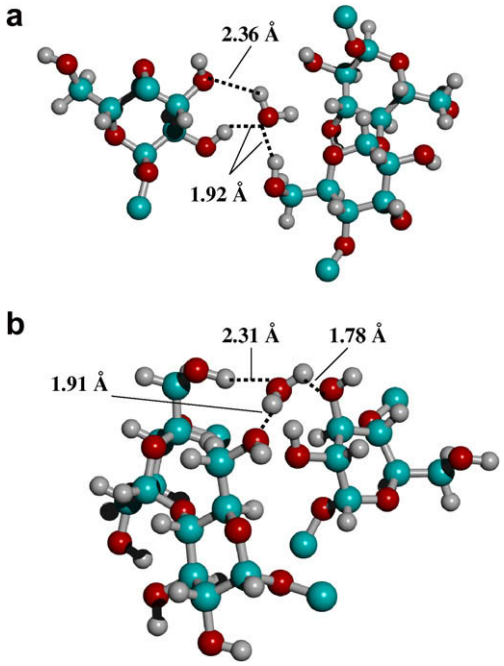

Fig. 3. (a) Water monomer ("bridging") interacting with H–O2, H–O3, and H–O6 of different residue segments stabilizing the different fragments of the amylase chain. (b) Water monomer ("bridging") interacting with H–O6 in consecutive residues, and H–O2 of different residue segments stabilizing the different fragments of the amylose chain.

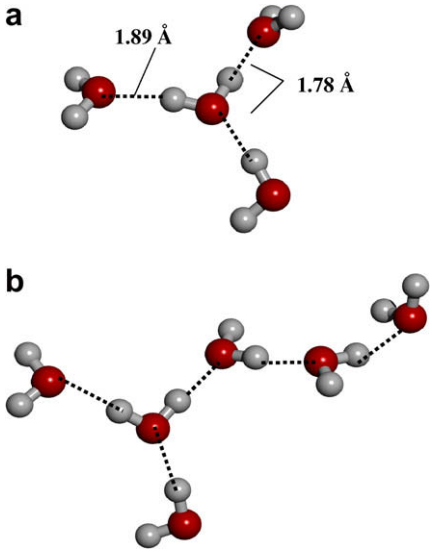

Fig. 4. (a) Water tetramer cluster. (b) Water hexamer cluster. Dashed lines show the water–water interactions.

acts as the central core water with three water molecules located around the central one. This is a special case of a small water cluster not directly interacting with the carbohydrate and this explains the near tetrahedral arrangement.

In Fig. 4b is shown a water cluster hexahydrate. This are defined as six water molecules hydrogen bonded together, not necessarily in a linear array. This complex cluster of six water molecules, contains three hydrogen bonds on one water molecule, two hydrogen bonds to the other two water molecules, and one hydrogen bond to the remaining water molecules. Fig. 5 shows water molecule interactions to c-DP-240, and it is clear that not all the water molecules in this cluster are interacting with the carbohydrate. It should be noted that some H···O distances between water and carbohydrate are fairly large (2.0–2.4 Å). In Fig. 6, a branched cluster of eight water molecules is shown. These water molecules are laid out between two amylose chains and have very good hydrogen bond lengths (1.8–2.0 Å). Four waters have no interactions within the cutoff distance with the amylose chains, thus one could suggest that they are stable in this cluster because of the water–water

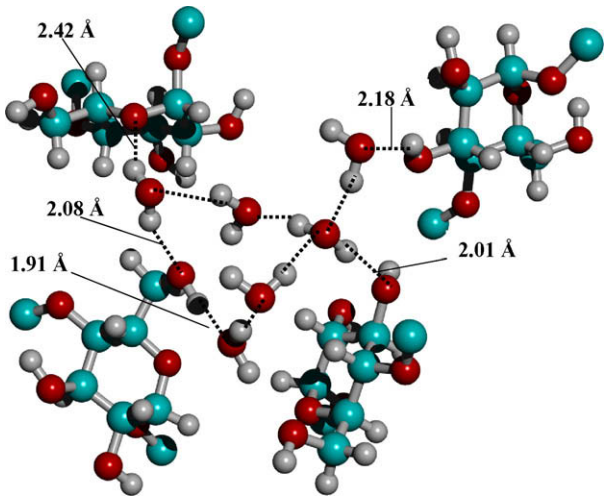

Fig. 5. Water hexamer cluster interacting with different fragments of the amylase chain.

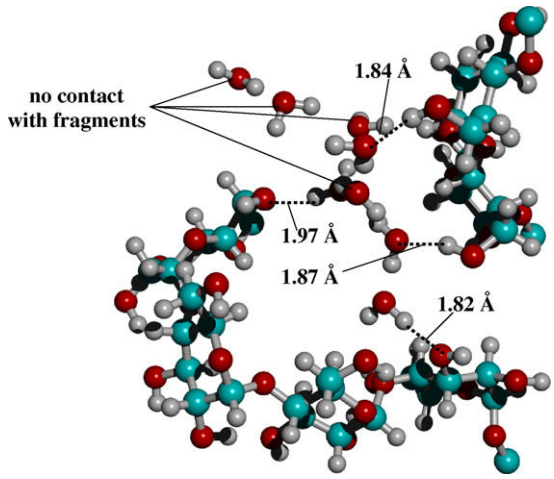

Fig. 6. Branched eight waters cluster interacting with different fragments of the amylose chain. Four of the eight waters in the cluster have no contact to the fragments.

interactions, completing a chain of water molecules supplying stability to the amylose lattice.

Finally, in Fig. 7a is shown an example of a large clusters, that is a cluster of 13 water molecules interacting with one another. As described before, several water molecules are not interacting with the carbohydrate, only with other water molecules as it is shown in Fig. 6. Some water molecules are not even close to the carbohydrate and could be considered as small water droplets with only surface interactions with the amylose matrix. These clusters are the closest representation of bulk water found in these simulations at the hydration level examined here. In Fig. 7b the largest water cluster found during the simulations is shown consisting of 29 water molecules. The interaction distance between waters in this cluster is found to be between 1.8 and 2.0 Å In all cases shown, the H–O···H angle made between water molecules is in agreement with high level theoretical studies of water-water and water–carbohydrates interactions (Momany & Willett, 2000b).

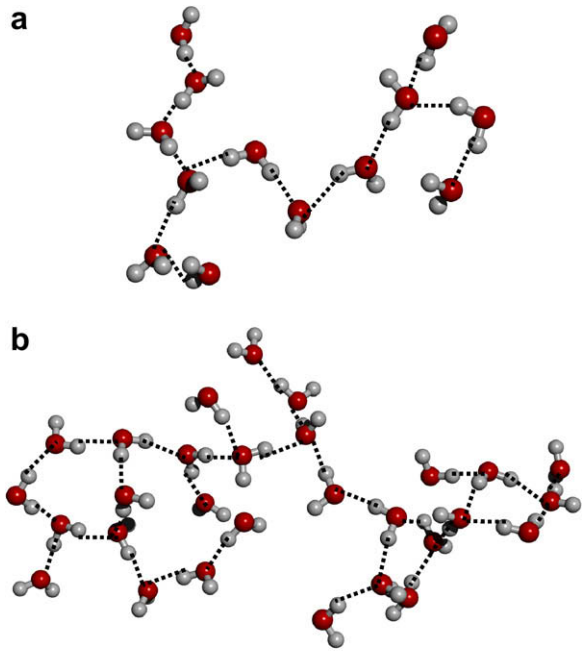

Fig. 7. (a) An example of larger water clusters during the simulations. Shown is a water cluster consisting of 13 water molecules. (b) Largest water cluster found during the simulations consisting of 29 water molecules. Dashed lines show the water–water interactions.

The self diffusion coefficients (D_T) of water in the c-DP-240 matrix are obtained from the slope of the mean square displacement versus time curves from Eq. (1). The diffusion values are obtained for different temperatures. Both the MSD per unit of time, and D_T values are given in Table 3. The D_T values range from a low of 0.00002 Å^2/ps for c-DP-240, to a value of ~0.06 Å^2/ps for the water molecules at temperatures above T_g. These results compare favorably with the experimentally measured diffusion coefficients of bulk water at different temperatures, that is, 0.114 Å^2/ps at 274 K to 0.358 Å^2/ps at 318 K (Mills, 1973). At 11% water/amylose the calculated D_T values are ~1/4 of the bulk water values. For example, the experimentally measured D_T value for water in a mixture of rhamnogalacturonan II (Monteiro and Herve du Penhoat, 2001), a 30 residue polysaccharide, is ~0.017 Å^2/ps at 298 K. This value is somewhat smaller than the values calculated here. The limited range for the experimental D_T values does not allow extrapolation to the higher temperatures, but one is satisfied that the calculated results are of the correct magnitude.

It is of interest to note the pattern of changes in D_T as a function of temperature. At temperatures lower than the glass transition temperature, T_g, value, the D_T values are generally lower than those at temperatures higher than T_g. Plotting T vs. D_T for c-DP-240 (see Fig. 8) we see that a change in slope occurs just above the T_g value for the concentration of interest. That implies that the translational diffusion of water in the matrix of amylose fragments is more difficult at temperatures below T_g and that water molecules travel more easily in the matrix for longer distances at any temperature above the T_g value. This appears to be intuitively correct but there is more to be learned from this data. The implication is that even though it is easier for a water molecule to move at the higher temperatures, they do not reach diffusion rates found in bulk water, even at temperatures significantly above T_g.

Plotting the natural log form of equation 2 (linear plot of lnD_T vs. 1/T) for the simulations at the 13% hydration level gave a value for the c-DP-240 activation energy of $\Delta E \sim 3.8$ kcal/mol. This value can be compared to the excess enthalpy of 2.79 kcal/mol for the concentration range of 1.9–9.1% and 1.24 kcal/mol for the range

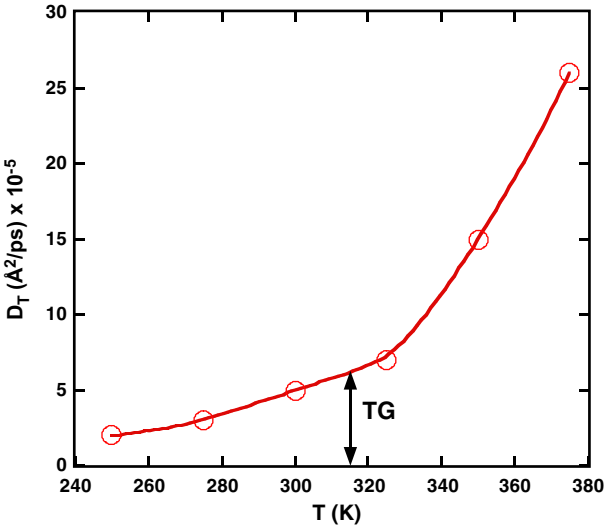

Fig. 8. Temperature (T) vs. self diffusion coefficients (D_T) for c-DP-240.

9.1–16% of water in native starch (Trommsdorff & Tomka, 1995b) and compares favorably with the energy of evaporation value of 3.4 kcal/mol for 8–14% water also reported (Trommsdorff & Tomka, 1995b) from calculations on starch models.

Examination of the movement of water molecules within the c-DP-240 cell showed that above T_g the water molecules generally vibrated within an approximately spherical volume (defined by the movement of the oxygen atom) ~2–3 Å in diameter. However, within the time frame of the simulation, it was generally found that the water molecule could migrate by small steps (~3–4 Å) to new positions in the cell. From Table 2 the calculated T_g values for the ~13% hydration level agree with the experimental values of 315–340 K. Further, it is clear that the movement of specific water molecules at the 250 K and 375 K simulations should differ at the two temperatures, and this is shown from the respective water diffusion coefficients at these temperatures, 0.02 and 0.07 $Å^2/ps^{-1}$ (see Table 3), respectively. When we examine the two temperature states, we find rather different water motion when defined as the distance from one oxygen atom (hydroxyl) attached to a specific glucose unit to a water oxygen atom, plotted as a function of the simulation time. At the lower temperature (i.e. 250 K), movement of the water (i.e. oxygen atom) relative to specific heavy atoms on the carbohydrate is ~1–2 Å or less, only rarely reaching values greater than 2 Å. On the other hand at 375 K the motion shows larger magnitude steps, ~2–3 Å, and migration to a new site through a series of consecutive steps, removed by ~5–7 Å from the original hydroxyl oxygen atom.

The density of starch like material is experimentally (Shogren, 2000) found to be in the 1.4–1.5 g/cm^3 range at hydration levels such as described here. It is of interest to examine the calculated values to find the reason for the low values (~1.30–1.35 g/cm^3) obtained here. A structural aspect of amorphous systems is the spatial distribution of interstitial holes or voids between molecules. Unoccupied volume can arise because of molecular packing defects, density fluctuations, or topological constraints. In calculations it can arise from defects in the molecular potentials (TIP3P water has a calculated density of 0.982 g/cm^3) (Jorgensen, Chandrasekhar, Madura, Impey, & Klein, 1983) or insufficient equilibration. A large void volume would suggest problems in one area or another. Previous studies (Kilburn, Claude, Schweizer, Alam, & Ubbink, 2005) have considered the void volume as one criterion for complete packing, but we will use thermodynamic properties which give 192 $Å^3$ to 197 $Å^3$ for the molar volume of glucose (Goldberg & Tewari, 1989). Correcting for a water molecule volume (Hough, Neidle, Rogers, & Troughton, 1973) of 27.4–30.7 $Å^3$/mol gives a value for a glycosyl residue of ~170 $Å^3$. When multiplied by 240 residues, a volume of ~41,000 $Å^3$ is found and adding the water volume for 297 water molecules of 8138–9118 $Å^3$ results in a total volume of ~50,000 $Å^3$. We compare this volume with the 300 K average volume of Table 1, 55605 $Å^3$, to give an excess or void volume of ~5500 $Å^3$ or ~10% of the calculated volume. Attempts to add new water molecules to the final cell after all the dynamics and temperature studies have been accomplished resulted in the addition of ~60–63 water molecules. The addition of 60 water molecules to the cell would result in the addition of ~2000 A^3 of volume, providing a correction of ~0.05 g/cc to the density. Note that when new water molecules are added to the cell, the hydration level changes and the T_g value changes, requiring complete recalculation of the volume, etc. Further, this addition of mass into void regions only accounts for ~1/2 of the missing mass or excess volume.

Another possible source for the calculated low density could be the large number of band-flip conformations in the c-DP-240 structure. If the volume the water molecules take around the normal *syn* conformation and the band-flip conformation (Gessler et al., 1999) differs, the overall volume for a given number of solvent molecules could differ, leading to an expanded volume for the band-flip conformation. This hypothesis was tested by carrying out PVT molecular dynamics simulations on a periodic cell of maltose in the normal and band-flip forms, with the box full of water. The resulting volume of the box reflects the difference in how the water molecules pack around the maltose molecule in the two conformations. Both simulations were started in the gg–gg–r conformation and remained so during 100 ps of dynamics at 300 K. The resulting averages showed that the band-flip conformer increased the volume of the cell by ~20 $Å^3$ per maltose molecule. If we now multiply the volume difference by the number of band-flips found in the c-DP-240, we have a correction factor to apply to the density found. This difference amounts to ~0.02 g/cc, and that is nearly sufficient to bring our corrected values (from filling holes with water molecules) up to the experimental values.

The above analysis suggests that the reason for the low density is in fact the number of band-flips the polymer undergoes as a result of trying to reduce the size of the periodic box. Each chain reversal creates less dense space than would be found experimentally in starch, that is, the persistence length of the amylose fragments in starch (i.e. several hundred Angstroms) is much larger than the maximum length available in our box (~60 Å diagonal length) and thus there are most probably many fewer chain reversals in native starch. We suggest that the number of chain reversals also contributes to the number of holes that can be filled with water molecules, a result of the many turns and band-flips the polymer must take to fit into the cell.

5. Summary

The preparation of the cell and calculation of T_g for amylose material is non-trivial, thus the strategy used to define the method, structure, and periodic cell are presented here in considerable detail. The generation of the c-DP-240 molecule is relatively easy, however, fitting the macromolecule into a periodic box small enough that simulations can be carried out in a reasonable period of time, is not particularly obvious or easy. Residue puckering from $^4C_1$ forms into boat forms during these calculations is addressed since these questions are not considered a problem when examining small sugar molecules simulations. Because of the stress placed on the chains to reverse direction to fit into the box, multiple high energy band-flip conformations were required along with kink forms. After the equilibrated box is obtained, and one has carried out successive tests with additional water molecules to fill void spaces, then production runs are prepared and volume trends examined. Only after the volume remains constant for significant simulation time is the system at near equilibrium.

After all the above difficulties are addressed, reliable data is obtained from the dynamic simulations. The calculated T_g values are in reasonable agreement with experimental values, and no serious deviations were found that would suggest that the calculated values were in question. Water clusters and diffusive movement were found to be consistent with experimental results and analysis of water clusters suggests that random dispersion of water molecules in the polymer matrix was obtained. The TIP3P water model give consistent results in good agreement with DFT studies (Momany & Willett, 2000b), and the empirical force field developed to study carbohydrates appears to work well for these very large systems. One test of this force field is presented in the Appendix, where a DP-26 structure determined from X-ray studies (Gessler et al., 1999) is used to test the parameters of the force field. In particular, the glycosidic bond dihedral angles are the primary determinates for the overall conformation, and these are well represented as shown in the Appendix.

Appendix A

Revised AMBER force field for starch like carbohydrates: AMB06C.

Atom types	
CS	Carbohydrate sp^3 6-membered ring carbon
CT	Hydroxymethyl carbon
AC	Alpha-anomeric carbon
AH	Hydrogen on alpha-anomeric carbon
OA	Alpha-anomeric bridge oxygen
OE	Carbohydrate ring ether oxygen
OT	Carbohydrate hydroxyl oxygen
OH	Hydroxymethyl oxygen
HO	Polar hydrogen on OH
HY	Polar hydrogen on OT or OA
HT	Hydrogen on CS
HC	Hydrogen on CT

Quadratic bond

i	*j*	Ro	*k*
AC	CS	1.509	365.0
AC	OA	1.400	334.3
AC	OE	1.394	250.0
AC	AH	1.090	340.3
CS	CS	1.496	365.0
CS	HT	1.090	324.3
CS	OA	1.406	334.3
CS	OE	1.400	296.7
CS	OT	1.420	285.0
CT	HC	1.090	339.0
CT	CS	1.483	365.0
CT	OH	1.410	324.0
HO	OH	0.966	460.5
HY	OA	0.972	475.5
HY	OT	0.966	476.5

Quadratic angles

i	*j*	*k*	θ	k–θ
AC	CS	CS	111.7	55.0
AC	CS	HT	108.72	37.0
AC	CS	OT	110.0	75.7
AC	OA	CS	114.7	62.0
AC	OA	HY	110.8	53.6
AC	OE	CS	111.9	62.7
AH	AC	CS	110.72	43.0
AH	AC	OA	109.89	45.9
AH	AC	OE	106.74	45.2
CS	AC	OA	105.0	75.0
CS	AC	OE	106.8	75.0
CS	CS	CS	110.7	55.0
CS	CS	CT	109.8	55.0
CS	CS	HT	108.72	40.0
CS	CS	OE	107.5	75.0
CS	CS	OT	108.0	75.7
CS	CT	HC	108.72	43.0
CS	CT	OH	108.0	75.7
CT	CS	HT	108.72	43.0
CT	CS	OE	104.0	75.0
CT	OH	HO	109.5	60.0
HC	CT	HC	109.5	37.0
HC	CT	OH	109.5	35.0
HT	CS	OE	109.24	52.0
HT	CS	OT	110.0	43.0
OA	AC	OE	111.0	92.3

Torsion 3-fold (missing force constant values are assumed to be 0.00, $\theta = 60$)

	i	*j*	*k*	*l*	k_1	θ_1	k_2	θ_2	k_3	θ_3
*	AC	CS	*					0.10		
*	AC	OA	*	1.2						
*	AC	OE	*					0.40		
*	CS	CS	*					1.28		
*	CS	CT	*					0.38		
*	CS	OA	*			4.6		0.50		
*	CS	OE	*					0.52		
*	CS	OT	*					0.15		
AC	CS	OT	HY	-0.6				1.05		
AH	AC	OA	CS	5.70	180.0					
AH	AC	OA	HY					0.45		
CS	AC	OA	CS			2.60	180.0			
CS	AC	OA	HY					0.40		
CS	AC	OE	CS					3.00		
CS	CS	AC	OE					3.00		
CS	CS	OT	HY					0.15		
HT	CS	CT	OT	1.40				0.58		
HT	CS	OA	AC					0.75		
OE	AC	OA	HY					0.40		
OE	AC	OA	CS					0.20		
OE	CS	CT	OT					0.58		

Non-bonded 6–12 terms

i	R_i (Å)	ε(kcal/mol)
AC	3.600	0.0903
AH	3.200	0.0045
CS	3.816	0.1094
CT	3.600	0.0600
HC	3.200	0.0045
HO	0.000	0.0000
HT	3.200	0.0045
HY	0.000	0.0000
OA	3.680	0.1650
OE	3.800	0.1650
OH	3.700	0.1650
OT	3.700	0.1650

1–4 Scaling = 0.75.

Atomic charges

Type	q(partial charge)	
CS	0.21	Hydroxyl groups (2,3-positions)
OT	−0.73	"
HY	0.535	"
HT	0.00	Hydrogen on CS
AC	0.53	1-position
OA	−0.64	Bridging oxygen
AH	0.00	Hydrogen on AC
OE	−0.63	Ether oxygen
CS	0.32	Next to OE at 5-position
CT	0.26	Hydroxymethyl
HC	0.05	Attached to CT
HO	0.53	Hydroxymethyl
OH	−0.71	"
CS	0.21	Bridge 4-position

A.1. Test of potentials

DP-26 (cyclomaltohexaicosaose) X-ray (Gessler et al., 1999) structure, averaged conformation over 102 ps steps, and energy

minimized at end of 102 ps molecular dynamics in a cubic periodic box of length 25 Å, 45 Å cutoffs, water molecules included to fill box. All atoms are included, hydrogen atoms added to heavy atoms and positions energy optimized. A dielectric of one is used with no added constraints. Hydroxymethyl and hydroxyl groups are originally positioned according to positions given in the X-ray structure paper (Gessler et al., 1999).

Res#	X-ray Structure		Average of 102ps molecular dynamics		Energy minimized from last ps frame	
	ϕ	ψ	ϕ	ψ	ϕ	ψ
1	90	-48	90	-53	97	-51
2	103	112	93	103	90	94
3	100	116	114	141	117	140
4	107	120	97	99	90	96
5	107	115	106	118	107	135
6	98	107	100	120	108	110
7	106	126	106	105	101	101
8	106	109	107	115	106	120
9	104	114	93	96	94	86
10	102	117	98	153	94	162
11	104	117	102	100	94	94
12	105	115	93	93	94	85
13	102	109	99	100	95	100
14	88	−50	95	−56	98	−51
15	106	123	101	163	91	−172
16	101	100	105	108	102	90
17	108	115	106	115	110	121
18	111	127	100	110	111	108
19	96	106	107	115	102	96
20	103	117	104	111	97	119
21	108	114	97	112	90	113
22	105	103	101	113	90	123
23	112	112	98	108	96	115
24	111	127	120	132	135	137
25	103	109	81	91	92	104
26	101	120	111	125	106	103
Ave.	104.5	114.6	101.6	110.3	100.5	110.0

ϕ(O5–C1–O1–C4') in degrees; ψ(C1–O1–C4'–C3') in degrees; average does not include band-flip values.

References

Accelrys Corporation, 9685 Scranton Road, San Diego, CA 92121-3752.

Astley, T., Birch, G. G., Drew, M. G. B., & Rodgers, P. M. (1999). Lifetime of a hydrogen bond to aqueous solutions of carbohydrates. *Journal of Physical Chemistry, A103*, 5080–5090.

Braesicke, K., Steiner, T., Saenger, W., & Knapp, E. W. (2000). Diffusion of water molecules in crystalline β-cyclodextrin hydrates. *Journal of Molecular Graphics and Modeling, 18*, 143–152.

Caffarena, E. R., & Grigera, J. R. (1997). Glass transition in aqueous solutions of glucose. Molecular dynamics simulation. *Carbohydrate Research, 300*, 51–57.

Caffarena, E. R., & Grigera, J. R. (1999). Hydration of glucose in the rubbery and glassy states studied by molecular dynamics simulation. *Carbohydrate Research, 315*, 63–69.

Ekdawi-Sever, N., Conrad, P. B., & de Pablo, J. J. (2001). Molecular simulation of sucrose solutions near the glass transition temperature. *Journal of Physical Chemistry, A105*, 734–742.

Goldberg, R. N., & Tewari, Y. B. (1989). Thermodynamic and transport properties of carbohydrates and their monophosphates: The pentoses and hexoses. *Journal of Physical Chemical Reference Data, 18*, 809–880.

Gessler, K., Uson, I., Takeshi, T., Krauss, N., Smith, S. M., Okada, S., et al. (1999). V-amylose at atomic resolution: X-ray structure of a cycloamylose with 26 glucose residues (cyclomaltohexaicosaose). *Proceedings of the National Academy of Science, 96*, 4246–4251.

Hough, E., Neidle, S., Rogers, D., & Troughton, P. G. H. (1973). The crystal structure of D-glucose monohydrate. *Acta Crystalgrafica, B29*, 365–367.

Howard, E. I., & Grigera, J. R. (1992). Conformations of erythritol and L-threitol in aqueous solution in relation to sweetness properties; A molecular dynamics simulation. *Journal of Chemical Society, Faraday Transactions, 88*, 437–441.

Hajduk, P. J., Horita, D. A., & Lerner, L. E. (1993). Picosecond dynamics of simple monosaccharides as probed by NMR and molecular dynamics simulations. *Journal of the American Chemical Society, 115*, 9196–9201.

Jorgensen, W. L., Chandrasekhar, J., Madura, J. D., Impey, R. W., & Klein, M. L. (1983). Comparison of simple potential functions for simulating liquid water. *Journal of Chemical Physics, 79*, 926–935.

Kilburn, D., Claude, J., Schweizer, T., Alam, A., & Ubbink, J. (2005). Carbohydrate polymers in amorphous states: An integrated thermodynamic and nanostructural investigation. *Biomacromolecules, 6*, 864–879.

Kullik, A. S., Chris de Costa, J. R., & Haverkamp, J. (1994). Water organization and molecular mobility in maize starch investigated by two-dimensional solid-state NMR. *Journal of Agricultural and Food Chemistry, 42*, 2803–2807.

Lee, S. L., & Debenedetti, P. G. (2005). A computational study of hydration, solution structure, and dynamics in dilute carbohydrate solutions. *Journal of Chemical Physics, 122*, 204511–204519.

Maler, L., Widmalm, G., & Kowalewski, J. (1996). Dynamical behavior of carbohydrates as studied by carbon-13 and proton nuclear spin relaxation. *Journal of Physical Chemistry, 100*, 17103–17110.

Mills, R. (1973). Self diffusion in normal and heavy water in the range 1–45°. *Journal of Physical Chemistry, 77*, 685–688.

Momany, F. A., & Willett, J. L. (2000a). Computational studies on carbohydrates: In vacuo studies using a revised AMBER force field, AMB99C, designed for α-(1 → 4) linkages. *Carbohydr Research, 326*, 194–209.

Momany, F. A., & Willett, J. L. (2000b). Computational studies on carbohydrates: Solvation studies on maltose and cyclomaltooligosaccharides (cyclodextrins) using a DFT/ab initio-derived empirical force field, AMB99C. *Carbohydrate Research, 326*, 210–226.

Momany, F. A., & Willett, J. L. (2000c). Computational studies on carbohydrates I. Density functional *ab initio* geometry optimization on maltose conformations. *Journal of Computational Chemistry, 21*, 1–16.

Momany, F. A., & Willett, J. L. (2002). Molecular dynamics calculations on amylose fragments. I. Glass transition temperatures of maltodecaose at 1%, 5%, 10%, and 15.8% hydration. *Biopolymers, 63*(9), 9–110.

Momany, F. A., Schnupf, U., Willett, J. L., & Bosma, W. B. (2007). DFT study of α-maltose: Influence of hydroxyl orientations on the glycosidic bond. *Structural Chemistry, 18*, 611–632.

Monteiro, C., & Herve du Penhoat, C. (2001). Translational diffusion of dilute aqueous solutions of sugars as probed by NMR and hydrodynamic theory. *Journal of Physical Chemistry, A105*, 9827–9833.

Orford, P. D., Parker, R., Ring, S. G., & Smith, A. C. (1989). Effect of water as a diluent on the glass transition behaviour of malto-oligosaccharides, amylose and amylopectin. *International Journal Biological Macromolecules, 11*, 91–96.

Parker, R., & Ring, S. G. (1995). Diffusion in maltose-water mixtures at temperatures close to the glass transition. *Carbohydrate Research, 273*, 147–155.

Perico, A., Mormino, M., Urhani, R., Cesaro, A., Tylianakis, E., Dais, P., et al. (1999). Local dynamics of carbohydrates. 1. Dynamics of simple glycans with different chain linkages. *Journal of Physical Chemistry, B, 102*, 8162–8171.

Roberts, C. J., & Debenedetti, P. G. (1999). Structure and dynamics of concentrated, amorphous carbohydrate-water systems by molecular dynamics simulation. *Journal of Physical Chemistry, 103*, 7308–7318.

Shimada, J., Kaneko, H., Takada, T., Kitamura, S., & Kajiwara, K. (2000). Conformation of amylose in aqueous solution: Small-angle X-ray scattering measurements and simulations. *Journal of Physical Chemistry B, 104*, 2136–2137.

Shogren, R. (2000). Modification of maize starch by thermal processing in glacial acetic acid. *Carbohydrate Polymers, 43*, 309–315.

Simperler, A., Kornherr, A., Chopra, R., Jones, W., Motherwell, W. D. S., & Zifferer, G. (2007). The glass transition temperatures of amorphous trehalose-water mixtures and the mobility of water: An experimental and in silico study. *Carbohydrate Research, 342*, 1470–1479.

Stevensson, B., Hoog, C., Ulfstedt-Jakel, K., Huang, Z., Widmalm, G., & Maliniak, A. (2000). Solid-state deuterium NMR and molecular modeling studies of conformational dynamics in carbohydrates. *Journal of Physical Chemistry, B104*, 6065–6070.

Tang, H.-R., Godward, J., & Hills, B. (2000). The distribution of carbohydrates in native starch granules-a multinuclear NMR study. *Carbohydrate Polymers, 43*, 375–387.

Trommsdorff, U., & Tomka, I. (1995a). Structure of amorphous starch. 1. An atomistic model and X-ray scattering study. *Macromolecules, 28*, 6128.

Trommsdorff, U., & Tomka, I. (1995b). Structure of amorphous starch. 2. Molecular interactions with water. *Macromolecules, 28*(613), 8–6150.

Tromp, R. H., Parker, R., & Ring, S. G. (1997). Water diffusion in glasses of carbohydrates. *Carbohydrate Research, 303*, 199–205.

Yoshioka, S., & Aso, Y. (2005). Comparison of the glass transition temperature and fragility parameter of isomalto-olygomer predicted by molecular dynamics simulations with those measured by differential scanning calorimetry. *Chemical Pharmacology Bulletin, 53*, 1443–1445.